NRIAG JOURNAL OF ASTRONOMY AND GEOPHYSICS
2025, VOL. 14, NO. 1, 1–17
https://doi.org/10.1080/20909977.2025.2460326

Siliciclastic reservoir characterisation and geometric trend modelling for hydrocarbon quantification and uncertainty analysis: a case study of Doma field, Niger Delta basin, Nigeria

Hammed Ajibola Oyesomi[b], Sunday Oladele[c], Kehinde Festus Oyedele[c], Adeogun Oluwakemi Yemisi[c] and Gabriel Efomeh Omolaiye[a]

[a]Department of Geophysics, University of Ilorin, Ilorin, Nigeria; [b]Halliburton Energy Services Nigeria Limited, Nigeria; [c]Department of Geoscience, University of Lagos, Nigeria

ABSTRACT

Reservoir architecture delineation and understanding of heterogeneity in geological reservoir models are crucial for accurately estimating hydrocarbon reserves, production forecast, and recovery in an effective economic scenario. This work demonstrates the combination of statistical tools and geometric trend models for hydrocarbon quantification and uncertainty analysis in the Doma Field development. 3D seismic cube and five (5) well data were integrated to build structure, facies, and petrophysical models (total and effective porosity, water saturation, net-to-gross, and permeability). Eleven (11) hydrocarbon-bearing reservoirs were identified and modelled out of twenty-two (22) reservoirs (sand 1–1B2–5-IB1) delineated and correlated from the logs. The saturation height function (SHF) was generated to populate the water saturation model to mitigate capillary pressure build-up. The structural model shows that fault-dependent three-way closure dominated the field. The results of petrophysical analysis and modelling biased to the litho-facies models indicated an average effective porosity value between 20 and 37% and water saturation ranging from 0.1 to 0.5. The permeability model showed that the permeability value was greater than 100 mD. Based on uncertainty analysis, the low case, base case, and high case cumulative volumetric for oil is 43.63MMSTB, 56.72MMSTB, and 71.34MMSTB and for gas is 73.65BSCF, 96.3BSCF, and 120.59BSCF, respectively. The coefficient of variation computed from log-derived porosity varies from 0.14 in reservoir 1-IB1 to 0.44 in reservoir 14-IB2. Also, the coefficient of variation computed from the 3D model porosity varies from 0.21 in reservoir 2-IB1 to 0.45 in reservoir 14-IB2. Thus, the research study has created a bridge between statistical tools in quantifying reservoir model heterogeneity and established a reference model for siliciclastic reservoir heterogeneity classification and prediction in the area and development of reservoir parameters in the adjacent areas of the Niger Delta basin.

ARTICLE HISTORY
Received 2 April 2024
Revised 15 December 2024
Accepted 15 January 2025

KEYWORDS
Modeling; structural interpretation; reservoir characterisation; seismic image; Niger Delta basin

1. Introduction

Commercial accumulation of oil and gas occurs in the Niger Delta province. The production of this commodity is derived from the pore spaces of reservoir rocks, primarily sandstone, which is distinguished by alternating layers of sandstone and shale units with thicknesses ranging from 100 to 1500 feet (30.48 m to 457.2 m) (Short and Stauble 1967; Doust and Omatsola 1990). Characterisation of reservoirs is in the vanguard of the energy shift, having progressed from its conventional function in petroleum exploration to becoming an essential component in the creation of subsurface energy solutions. The technique of systematically integrating various data types and quantities to depict reservoir properties of relevance in inter-well locations is known as reservoir characterisation (Ezekwe and Filler 2005). The characterisation framework for comprehending the intricate subsurface systems that will power our future is aided by the integration of several disciplines, ranging from geophysics and geology to petrophysics and reservoir engineering (Bedle et al. 2024). The main goals of any reservoir characterisation are to provide information, encourage trust, and offer usefulness. It must be reliable enough to be consulted, which will eventually lead to better choices and results in the future (Weston 2024). However, the objective of any reservoir modelling and characterisation is to integrate data from various sources in order to comprehend reservoir connectivity in both static and dynamic situations. Seismic attribute analysis has been and continues to be pertinent in the generation of the framework of the reservoir model (Meldahl et al. 2001). Not only are three-dimensional geological reservoir modelling and integrated reservoir characterisation essential for describing and predicting oil reserves in reservoirs, but also an essential means to quantitative characterisation of reservoir structure architectural geometry

CONTACT Gabriel Efomeh Omolaiye gab_omolaiye@yahoo.co.uk Department of Geophysics, University of Ilorin, Ilorin, Nigeria

and heterogeneity in three-dimensional space, and its core is to predict hydrocarbon volumetric distribution within the reservoir (Oladele et al. 2020). Therefore, reservoir modelling represents the major focus of hot topical issues in reservoir geoscience. Three-dimensional modelling of a reservoir is a process of selecting appropriate methods to establish the structure, sedimentary microfacies, sand body geometry, and reservoir petrophysical parameters based on well logging, seismic, and geological data.

Trend heterogeneity in reservoir study means the vertical and lateral variation in porosity, permeability, and/or capillarity. In the Niger Delta province of Nigeria, hydrocarbon is accumulated in the intercalated sand and shale of Agbada Formation. The existence of fractures and faults, diagenesis, and variations in the depositional environment and facies are some of the common causes of the reservoir trend heterogeneity in sandstone bodies, which can occur at different lengths and scales from micrometres to hundreds of metres (De Ros et al. 1998, Schulz – Rojahn et al.; 1989 Ekwenye et al. 2015). Thus, understanding and forecasting reservoir heterogeneity is crucial for developing and implementing effective plans for producing hydrocarbons (Hamilton et al., 1998, Barton et al. 1992; Sech et al. 2009). The shape and internal structure of the sand bodies, grain size, level of bioturbation, provenance, and the kind, volume, and distribution of diagenetic alteration all affect the trend heterogeneity pattern of sandstone reservoirs, which in turn controls the volume, flow rate, and recovery of hydrocarbons. Ulisses Miguel Correia et al. (2016) worked on 3-D Geological modelling: a siliciclastic reservoir case study from Campos Basin, Brazil. In the study, they stated that Dykstra–Parsons's coefficient takes values between 0 and 1 and, for most reservoirs, this coefficient ranges between 0.5 and 0.9, from homogenous to heterogeneous. They concluded that a Dykstra-Parsons coefficient of V = 0.52 characterises this reservoir as moderately homogeneous. In 2017, Marinovska and IIieva established that the 3D Reservoir Modelling process and Simulation is a reliable reflection of the real geological situation and its dynamic changes within the hydrocarbon field. Adepelumi et al. (2018) attempt the construction of a 3D reservoir model that characterises the XYZ field of Niger Delta Province and evaluates its hydrocarbon production performance. The research showed the efficacy of 3D reservoir modelling technology in understanding the spatial distribution of petrophysical properties and providing a framework for future production performance behaviour of XYZ field, Niger Delta.

Fitch et al. (2015) established that basic statistics can be used to characterise variability in a dataset, in terms of the amplitude and frequency of variations present. A better approach involves heterogeneity measures since these can provide a single value for quantifying the variability and provide the ability to compare this variability between different datasets, tools/measurements, and reservoirs. Dykstra and Parsons (1950) developed a criterion for quantifying reservoir heterogeneity based on the permeability distribution and the well-known coefficient of variation. Dykstra-Parsons coefficient takes values between 0 and 1 and, for most reservoirs, this coefficient ranges between 0.5 and 0.9, from homogenous to heterogeneous. Another geostatistical tool used in quantifying heterogeneity in reservoirs is the coefficient of variation. Also known as relative standard deviation, the coefficient of variation is a statistical concept that accounts for relative variability in the data set. It is the ratio of the standard deviation to the mean. The higher the coefficient of variation, the greater the level of dispersion around the mean and the higher the intraformational heterogeneity nature of the reservoir. The lower the coefficient of variation, the more homogenous is the reservoir (Elkateb et al. 2003).

This research focused on the delineation of the architectural geometry of the sand body, geologic and 3D static modelling, and evaluation of the field siliciclastic reservoir heterogeneity for hydrocarbon quantification and uncertainty analysis, it will also serve as a reference model for reservoir heterogeneity prediction in the area and development of reservoirs parameters in the adjacent areas of the Niger Delta basin.

2. Regional geology of Niger Delta

Numerous scholars have studied the Niger Delta's geology. Short and Stauble (1967) discuss the stratigraphic development of the Cretaceous strata underneath and the Tertiary Niger Delta. Tuttle et al. (1999), Doust and Omatsola (1989), Okeke and Umeji (2016) and Evamy et al. (1978) provide descriptions of the petroleum geology of the Niger Delta. Using sequence stratigraphic approaches, Stacher (1995) created a hydrocarbon habitat model for the Niger Delta. The physiography, sedimentation, and depositional settings of the contemporary Niger Delta were characterised by Allen (1965) and Oomkens (1974). The Akata, Agbada, and Benin formations (Figure 1), the three main lithostratigraphic units described in the Niger Delta subsurface, decrease in age basinward, representing the general regression of depositional conditions inside the Niger Delta clastic wedge (Agharanya et al. 2022). In southern Nigeria, there are exposed stratigraphic equivalent units to these three formations.

The formations show a progradational clastic wedge that is grossly coarsening upward in a marine, deltaic, and river setting (Short and Stauble 1967; Weber and Daukoru 1975; Weber 1987). According

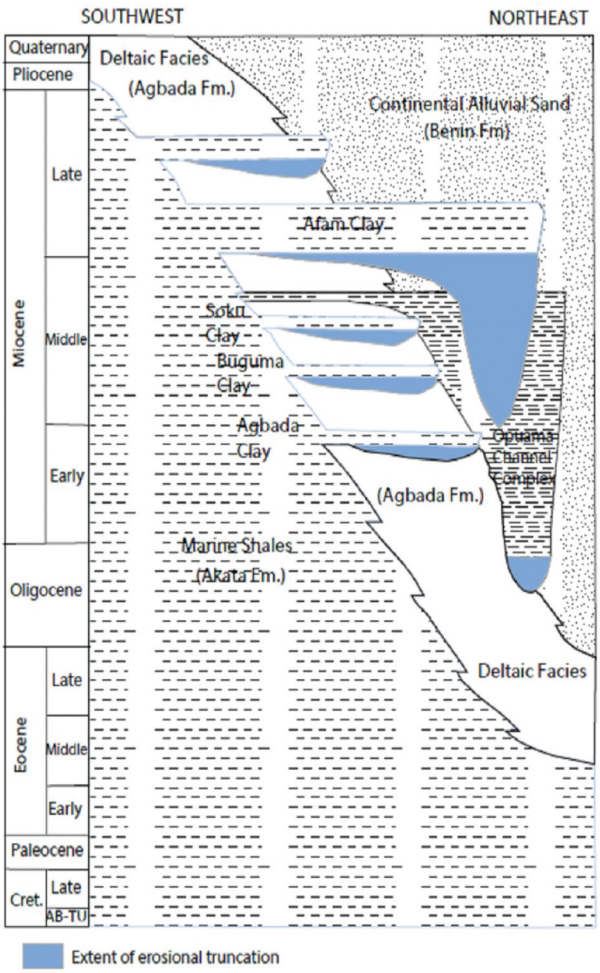

Figure 1. Stratigraphic column showing the three formations of the Niger Delta (Doust and Omatsola 1989).

to Short and Stauble (1967), the Akata Formation's type section was identified at the Akata 1 Well, which is located 80 km east of Port Harcourt. A total depth of 11,121 ft (3,680 m) was reached in the Akata 1 well without encountering the base of this formation.

The deepest occurrence of deltaic sandstone strata (7,180 ft (2189 m)) in the Akata well defines the top of the formation. In the centre of the clastic wedge, the thickness of the formation is estimated to be 21,000 feet (6300 metres). Dark grey shales and silts make up the lithologies, with sporadic sand streaks that are likely the result of turbidite movement. Up to 50% of the microfauna collection is composed of marine planktonic foraminifera, which indicates shallow marine shelf deposition (Doust and Omatsola 1989; Ekwenye, 2015). These shales are thickest along the axis of the Benue and Bida Troughs, having been created during the early stages of Niger Delta progradation. This formation is known as the Imo Shale when it is exposed onshore in northeastern Nigeria. Moreover, the formation appears offshore along the continental slope in diapirs. These marine shales are usually overpressured when firmly buried. Stacher (1995) concluded that the Akata shales were deposits from the Deepwater low stand. According to Doust and Omatsola (1989), the formation grades vertically into the Agbada Formation, with a large amount of plant remnants and micas in the transition zone. The formation can be found throughout the clastic wedge of the Niger Delta, with a maximum thickness of about 13,000 feet (3962.4 m). In southern Nigeria, where it appears (between Ogwashi and Asaba), it is called the Ogwashi-Asaba Formation (Doust and Omatsola 1989). Sands, silts, and shales alternate in the lithologies, which are characterised by gradual increases in grain size and bed thickness and are grouped in successions ranging from ten to several hundred feet. The majority of interpretations place the strata's formation in fluvial-deltaic settings. The Agbada Formation lies between Eocene and Pleistocene in age.

According to Short and Stauble (1967), the Benin Formation is the uppermost portion of the Niger Delta clastic wedge, extending from the northern Benin-Onitsha region to beyond the current shoreline; this was observed in the Elele 1 well (type well), located roughly 38 km to the northwest of Port Harcourt. The base of the formation reaches a depth of 4600 feet (1402 metres), with the most recent subaerially visible delta top surface at its peak. The youngest marine shale defines the base. According to Doust and Omatsola (1989), non-marine sand that was deposited in the upper coastal plain or alluvial habitats during the delta's progradation makes up the entirety of the formation's shallow portions. The age of the formation is considered to range from Oligocene to Recent, although the paucity of surviving fauna prevents exact age dating (Short and Stauble 1967). The formation finishes close to the shelf margin and thins basinward. The coastal plain and shallow marine sandstones are interspersed with broad bands of continental deposits that make up the Benin Formation. The formation water is fresh with high resistivity.

2.1. Location of research area

The Doma field is situated in the eastern part of the offshore Niger Delta Basin. This consists of several regional deposition belts each subdivided into "macrostructures" defined by large, listric, and synsedimentary, south-dipping normal faults. The study area is a green field and non-producing, the five wells that penetrated fields were used for this study (Figure 2).

3. Materials and methodology

3.1. Materials

The data used for this study comprise 3D seismic data covering an area of about 6424.0178 acres and suites of composite well logs (GR, ILD, NPHI, RHOB),

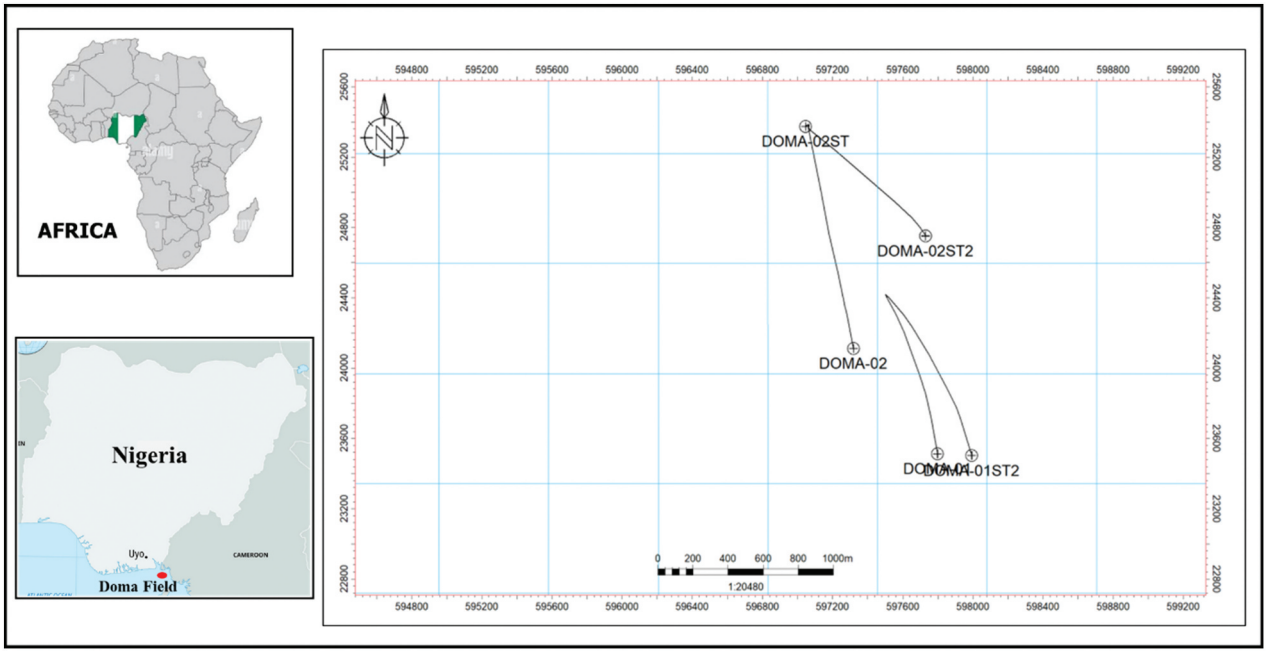

Figure 2a. The basemap of the study area offshore Niger Delta.

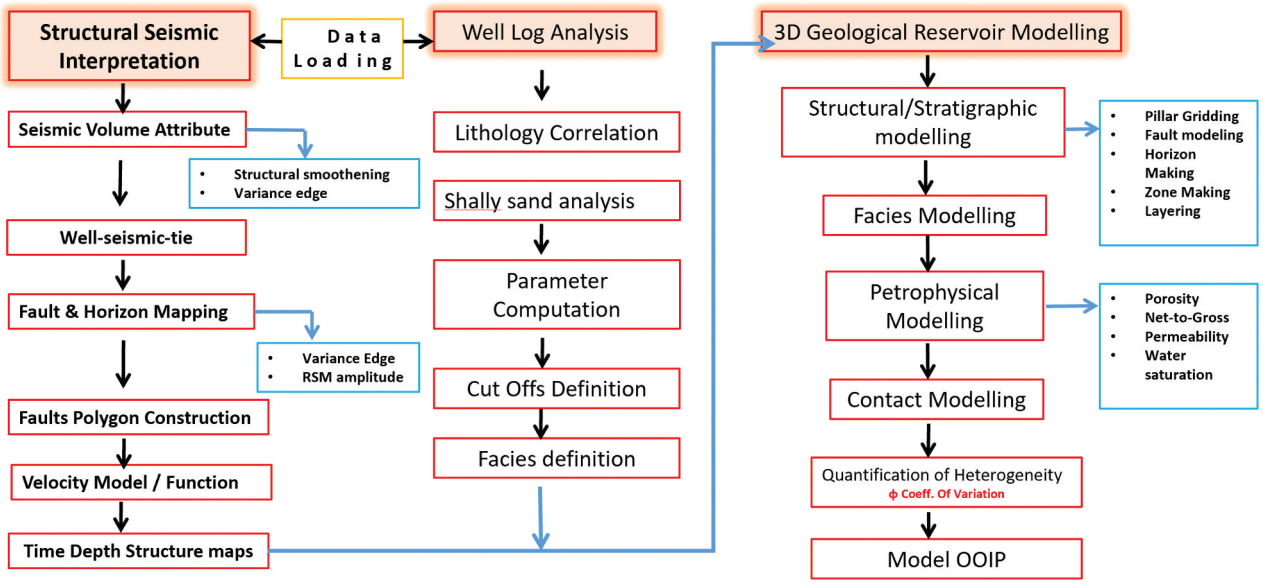

Figure 2b. Integrated methodology adopted.

deviation data, and check-shot data from five (5) wells (Doma 1, Doma 1st2, Doma 2, Doma 2st1, and Doma 2st2). The base map of the study area is shown in Figure 2a.

3.2. Methodology

The integrated methodology (Figure 2b) adopted during this research utilised industry-based tools and processes to ascertain the objectives of this study. Reservoir identification and estimation of petrophysical properties were done using the TECHLOG™ tool under the Petrophysics module. Reconnaissance seismic interpretation and finely gridded high-resolution 3D geological static reservoir model of the field was built and the volume of hydrocarbon in place was evaluated using the PETREL™ tool under geoscience core bundles which consist of seismic interpretation, structure and stratigraphic modelling, facies modelling, petrophysical modelling, and uncertainty analysis module. Microsoft Excel was used for the statistical analysis in the quantification and classification of the type of heterogeneity that characterise the study area.

3.3. Petrophysical analysis

The electronic logs in LAS/ASCII format were imported into TECHLOG software after the proper quality check was done. This was done to make sure that throughout data transmission, the imported log data were not tampered with. When necessary, logs were examined and depth matched. The proper TECHLOG procedure was followed to harmonise dataset names and allocate them to the appropriate families and units. The primary depth reference for each well was the first Gamma Ray log run. The refined and processed logs were employed in the creation of finely gridded three-dimensional static reservoir models as well as in geological and petrological studies. The correlated reservoir of interest throughout the Doma field is depicted in Figure 3.

3.4. Determination of petrophysical parameters

The petrophysical analysis was done using all the available well data. Petrophysical parameters such as Volume of Shale, Total and Effective Porosity, Water saturation, and detailed methodology were adopted in the analysis. Figure 4 shows the evaluation log plot of some reservoirs in the Doma field.

3.5. Reconnaissance seismic interpretation

The seismic volume was imported into a user-defined folder in SEG-Y; this was done by quality-checking the data and making sure the correct bytes were used in loading. After loading into memory, a time slice was also inserted. Well data were also loaded into the software and a proper quality assessment was done (Figure 5a). This is to allow the visualisation of these wells at their different locations within the survey area. Structural Smoothening and Variance edge volume attributes were applied to enhance fault identification and mapping (Figures 5b, c).

3.6. Seismic to well tie

To link geology observed/interpreted log data with seismic events, a well-to-seismic connection was implemented (i.e. correlation of formation tops and seismic reflectors). Seismic interpretation benefits greatly from reliable and precise well ties. Seismic "loops" or wiggles develop into geologic interfaces that have stratigraphic and lithologic significance. Conversely, petrophysical and stratigraphic observations based on log data sonic and density logs required for synthetic seismogram were quality checked and edited where necessary, and sonic calibration was done using available checkshot data. An analytical wavelet (Ricker) with a dominant frequency of 28 hz was used in the synthetic seismogram generation. No bulk shift was performed for any of the wells, but reasonable stretch and squeeze were performed where necessary, without distorting the interval velocity so that the synthetic seismogram reflectors is manually matched to real seismic data. The Doma 2 synthetics were matched with seismic volume and integrated with gamma ray and resistivity log and the result of the synthetic seismogram is displayed in the Figure 5b below.

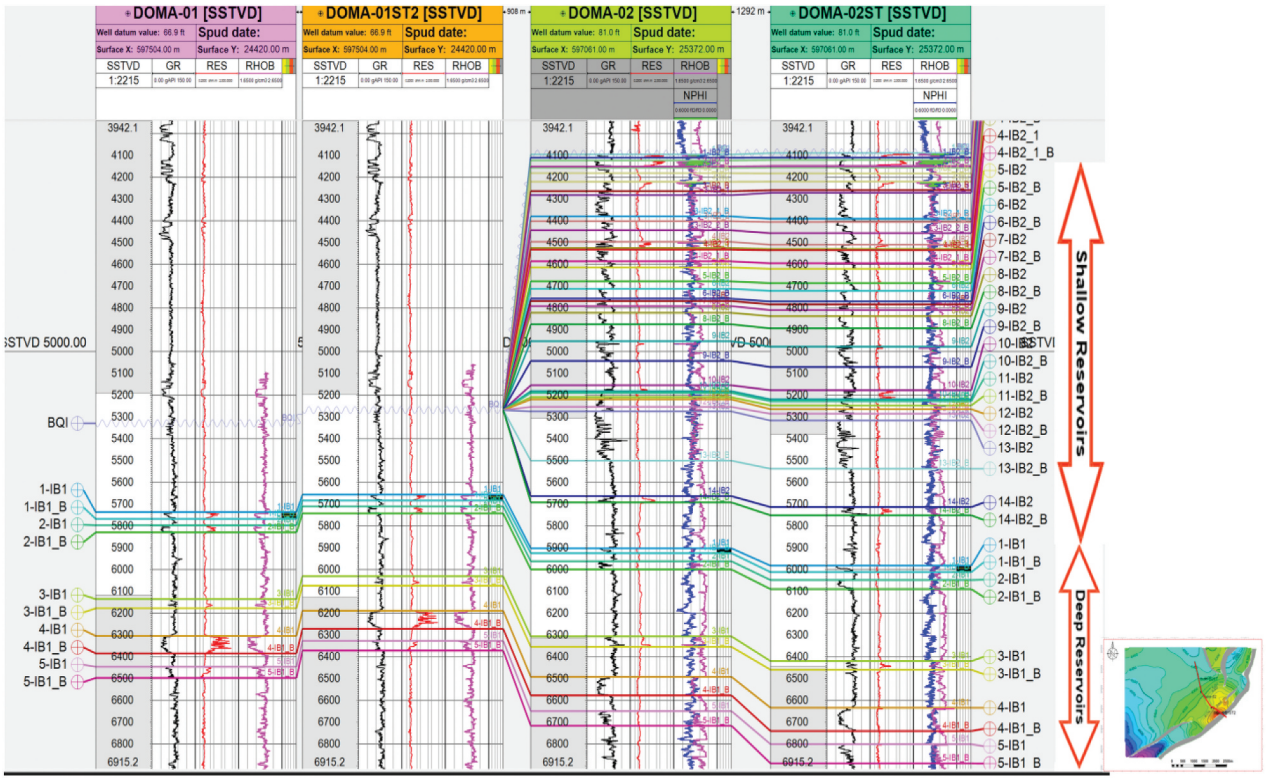

Figure 3. Showing Correlation of Reservoirs of interest in all wells within the Doma field.

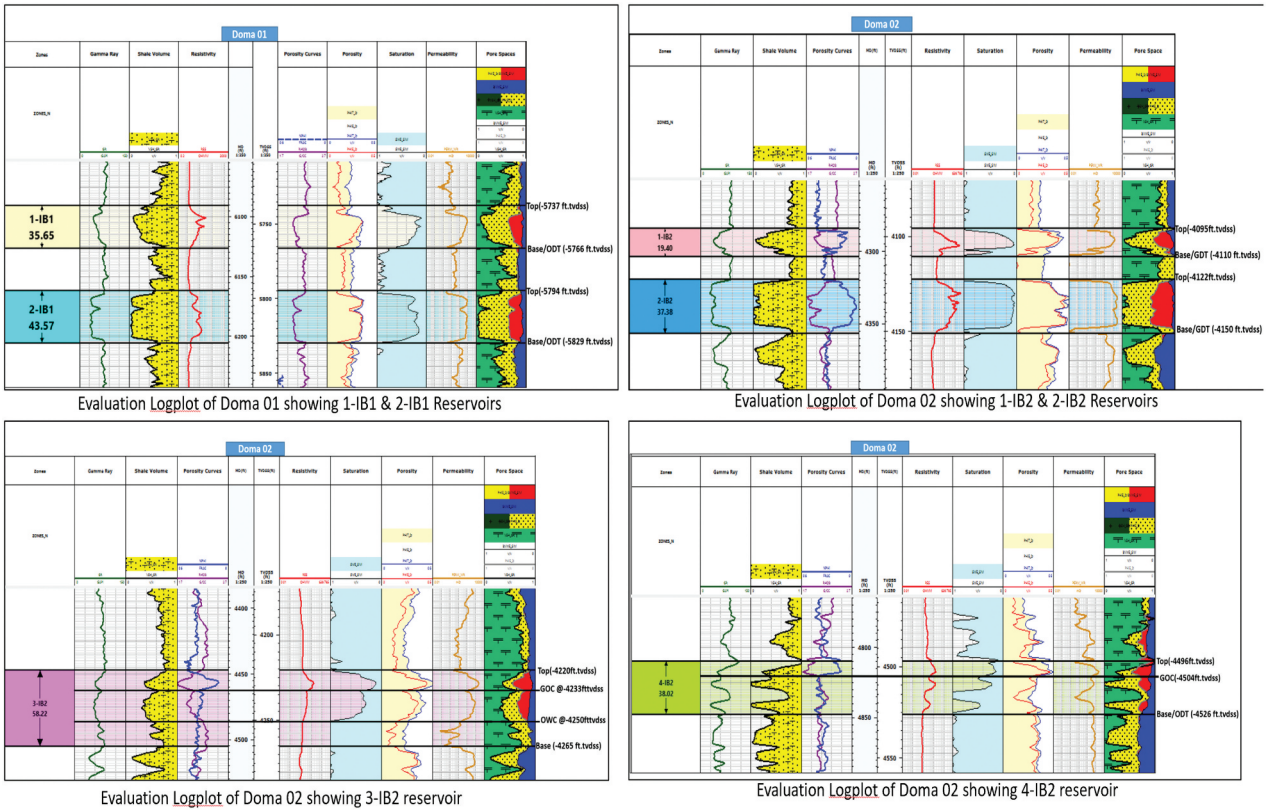

Figure 4. Showing evaluation log plot of some reservoirs in wells within the Doma field.

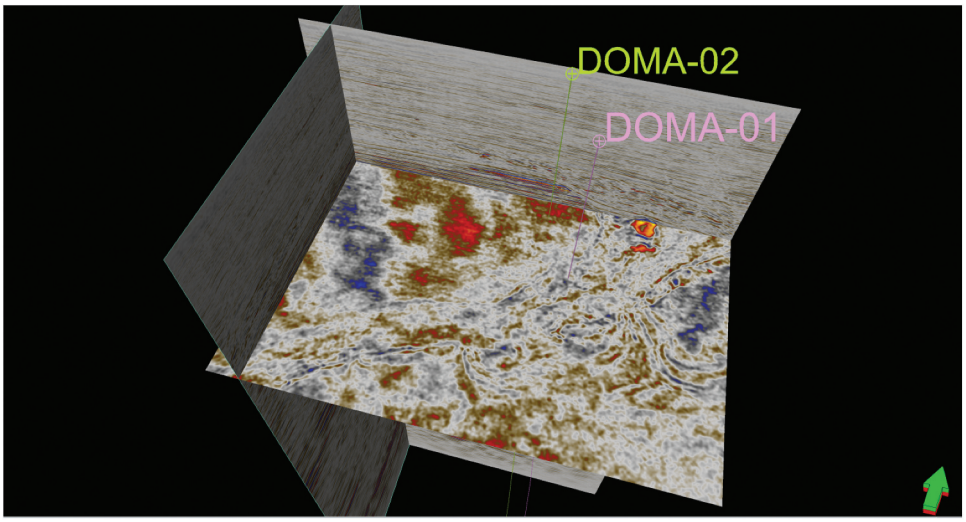

Figure 5a. Showing inline, crossline, time slice, and some wells available for the study.

3.7. Horizon mapping

After establishing well to seismic tie using the available check shot and synthetic seismogram, the reservoir tops were displayed on seismic sections. Eleven (11) hydrocarbon-bearing horizons were interpreted for the structural definition of the Doma field. These horizons include the Base of Qua Iboe (BQI) and seven of the hydrocarbons bearing levels (2-IB2, 3&4-IB2, 5-IB2, 6-IB2, 1&2-IB1, 3-IB1 and 4&5-IB1). Horizon interpretation was carried out manually at an interval of every 8 lines. Interpreted horizons were gridded with Petrel's "Make/Edit Surface" utility. The horizons mapped on both crossline and inline (Figure 5c) were used to generate a 3-D grid time map.

3.8. Time-to-depth conversion

A depth conversion model for the Doma field was created using the 3rd-order polynomial function. The velocity function was created from the available Doma 1 well check-shot. The available Doma-1 well check-shot was plotted, and a line of best fit was taken.

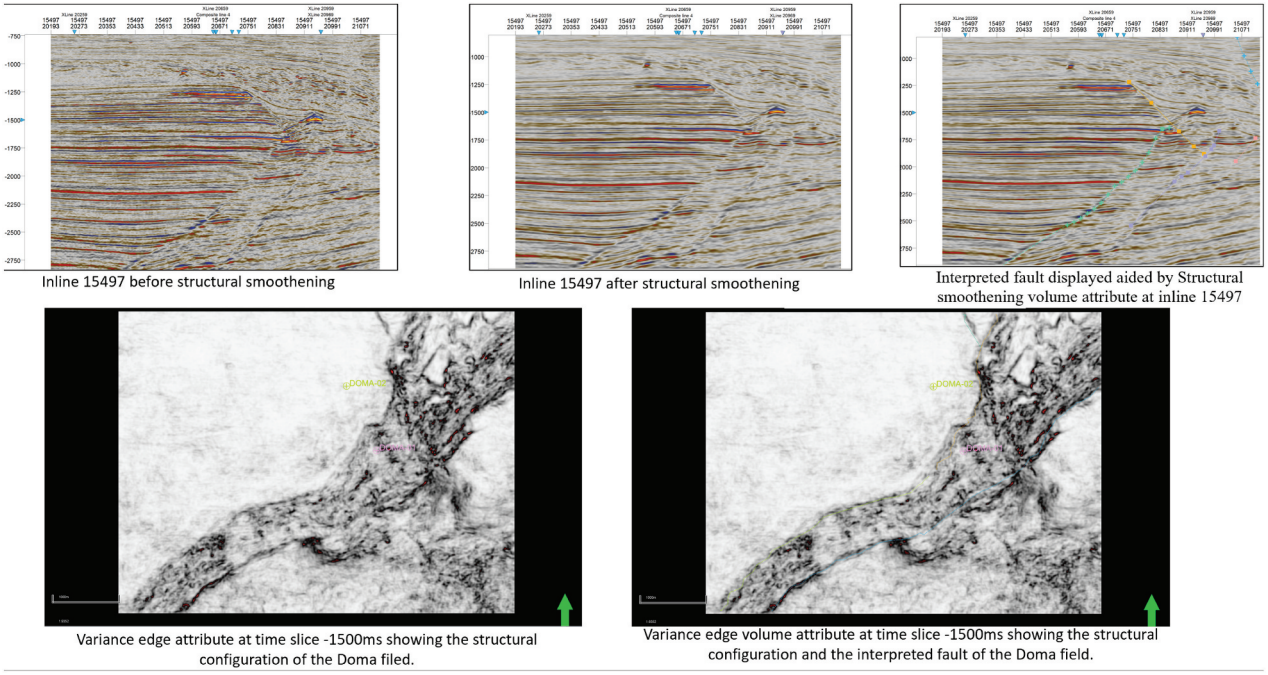

Figure 5b. Showing structural smoothening and Variance Edge seismic volume attribute in the study area.

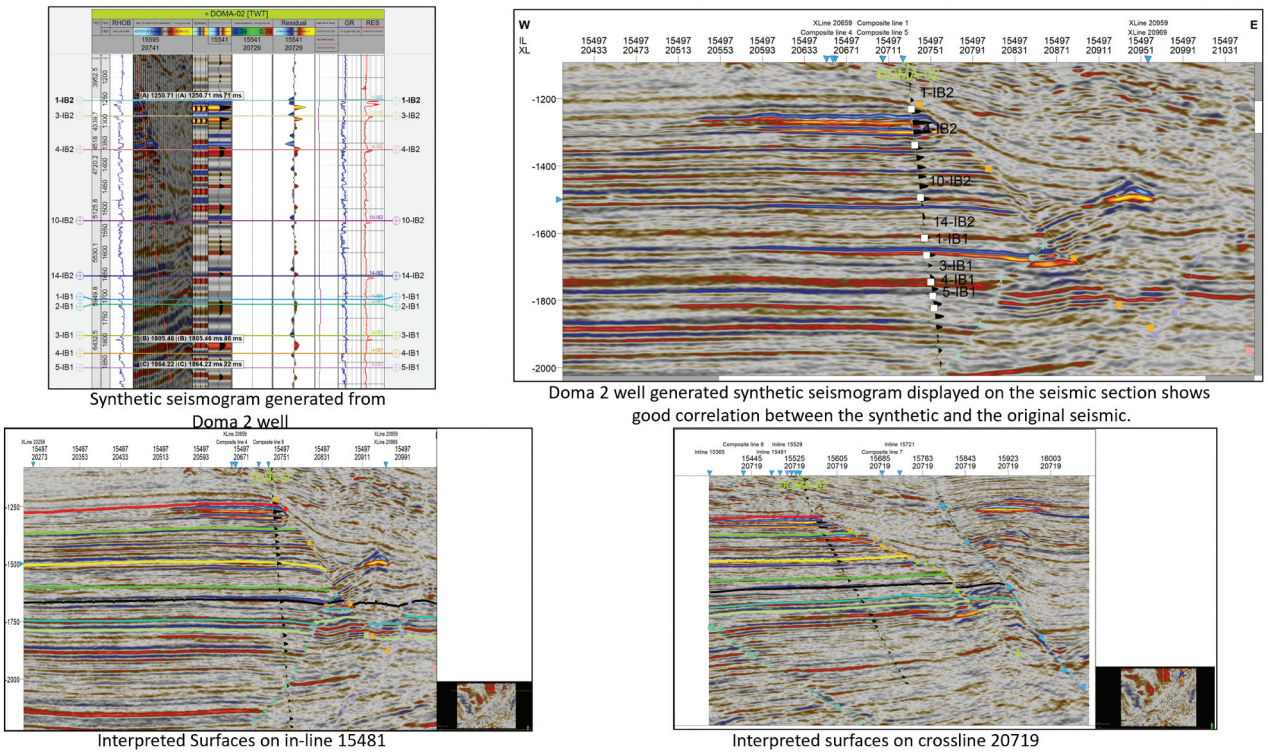

Figure 5c. Showing synthetic seismogram, and Horizon interpretation in Doma Field.

The resultant equation was then used to calculate a correspondent depth for the given two-way time. Final depth maps were calibrated to Doma well tops by vertical shift (Figure 5d).

3.9. 3D geological static reservoir modelling

The geological 3D static model was built by integrating relevant subsurface information and data. Results of seismic reconnaissance survey and structural interpretation, lithology description, litho-facies interpretation, and petrophysical analysis (effective porosity, permeability, water saturation, net-to-gross) were all incorporated to build the 3D static model in Petrel software to establish the 3D structure architectural geometries of reservoirs and delineate heterogeneity that represent as closely as possible the subsurface reality within Doma field.

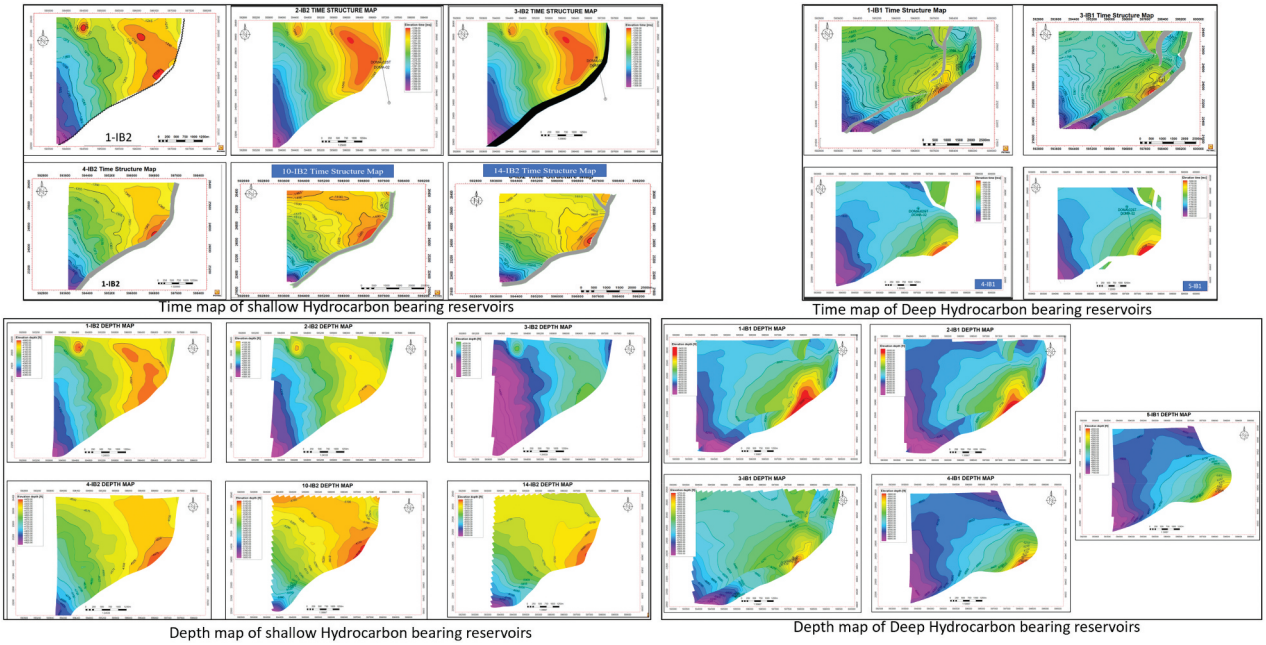

Figure 5d. Showing Time and Depth maps for all hydrocarbon bearing levels in Doma Field.

The objectives of the integrated geological 3D static reservoir modelling are but are not limited to the following:

- Build finely gridded, faulted 3D static model of the 1-IB2, 2-IB2, 3-IB2, 4-IB2, 10-IB2, 14-IB2, 1-IB1, 2-IB1, 3-IB1, 4-IB1 and 5-IB1 reservoirs in Doma field,
- Distribute litho-facies and petrophysical properties,
- Establish the petrophysical trend within the models that characterise the field,
- Calculate the volume of oil and gas within the field.

3D static models were built for 1-IB2, 2-IB2, 3-IB2, 4-IB2, 10-IB2, 14-IB2, 1-IB1, 2-IB1, 3-IB1, 4-IB1, and 5-IB1 reservoirs to delineate Doma field heterogeneity, characterise reservoirs within the field, support hydrocarbon volumetric assessment for field performance prediction.

The model is primarily built based on inputs from seismic, geological, and petrophysical evaluation processes described in the previous section of this research. The Schlumberger 3D static modelling workflow was adopted in building the 3D geological reservoir models for the probable hydrocarbon-bearing reservoir within the Doma field.

3.10. 3D structural grid design and modeling

The grid cells were set at 100 × 100 * 2 along I, J, and K directions, respectively, considering the areal extent of the field and thickness of the reservoirs. The three-dimensional structural grid was constructed with a combination of the fault network and seismic horizons. Fault modelling is the determination of the different faults in the model that served as the foundation for creating the 3D grid. The reservoirs within the Doma field are bounded by Northeast Southwest trending synthetic growth fault, which is the major fault within the field. There are other smaller synthetic faults observed in the deeper reservoirs. The lateral shape and geometry of these faults were defined by modelling. The 3D structural framework of Petrel software was based on the horizon and the modelled faults (Figure 6). The faults were built using key pillars and were constantly checked with the surfaces so as not to deviate from the original geometry of the fault (Figure 6). Fault Modelling was carried for all the shallow reservoirs (1-IB2, 2-IB2, 3-IB2, 4-IB2, 10-IB2, 14-IB2) (Figure 6) and deep reservoirs (1-IB1, 2-IB1, 3-IB1, 4-IB1 and 5-IB1) (Figure 6) reservoir models. The modelled faults were then quality checked to ensure they accurately represent the input data and interpretation of 1-IB2, 2-IB2, 3-IB2, 4-IB2, 10-IB2, 14-IB2, 1-IB1, 2-IB1, 3-IB1, 4-IB1, and 5-IB1 structures as shown in Figure 6.

3.11. Vertical layering

Vertical layering of reservoirs 1-IB2, 2-IB2, 3-IB2, 4-IB2, 10-IB2, 14-IB2, 1-IB1, 2-IB1, 3-IB1, 4-IB1 and 5-IB1 3D grids were carried out by using:

(1) Main reservoir layers from seismic interpretation
(2) Zonations/Isochores maps from geological interpretation and
(3) Final vertical cell resolution defined by cell thickness/number of cell layers.

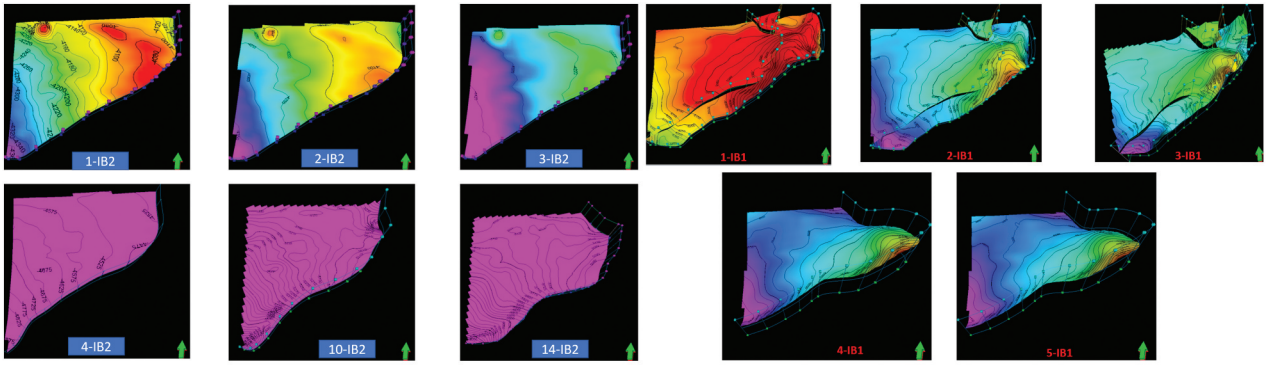

3D display of modelled faults with 1-IB2, 2-IB2, 3-IB2, 4-IB2, 10-IB2 & 14-IB2 top & base surfaces

3D display of modelled faults with 1-IB1, 2-IB1, 3-IB1, 4-IB1, & 5-IB1 top & base surfaces

Figure 6. 3D display of modelled faults with top & base surfaces in Doma Field.

Cell thickness was determined by rounding to the nearest whole number the result of dividing the maximum observed well isochore of the zone by 2 ft.

3.12. Horizontal variogram analysis

A Variogram map (Figure 7) was generated from the porosity trend map to determine the major and minor directions of anisotropy. Sample Variograms for the major and minor directions were then computed. The orientation was defined using the anisotropy direction values derived from the Variogram map. Finally, a Variogram model was matched with the sample Variogram to create a best-fit model Variogram curve. Different ranges in Major and Minor directions are indicative of geometric anisotropy. The major axis is 5600, the minor is 3000 and the angle/azimuth is 45 degree (Figure 7). These were used as input in litho-facies and the petrophysical modelling process.

3.13. Scale up well logs

The scale-up well logs process averages the values of the logs penetrated by wells to the cells in the 3D grid. Each cell gets one value per up-scaled log. These cells are later used as a starting point for property modelling (Schlumberger 1989). When modelling electro-facies/litho-facies and petrophysical properties, a 3D grid cell structure is used to represent the volumes of the zones. The cell thickness will normally be larger than the sample density for well logs. As a result, the well log must be scaled up to the resolution of the 3D

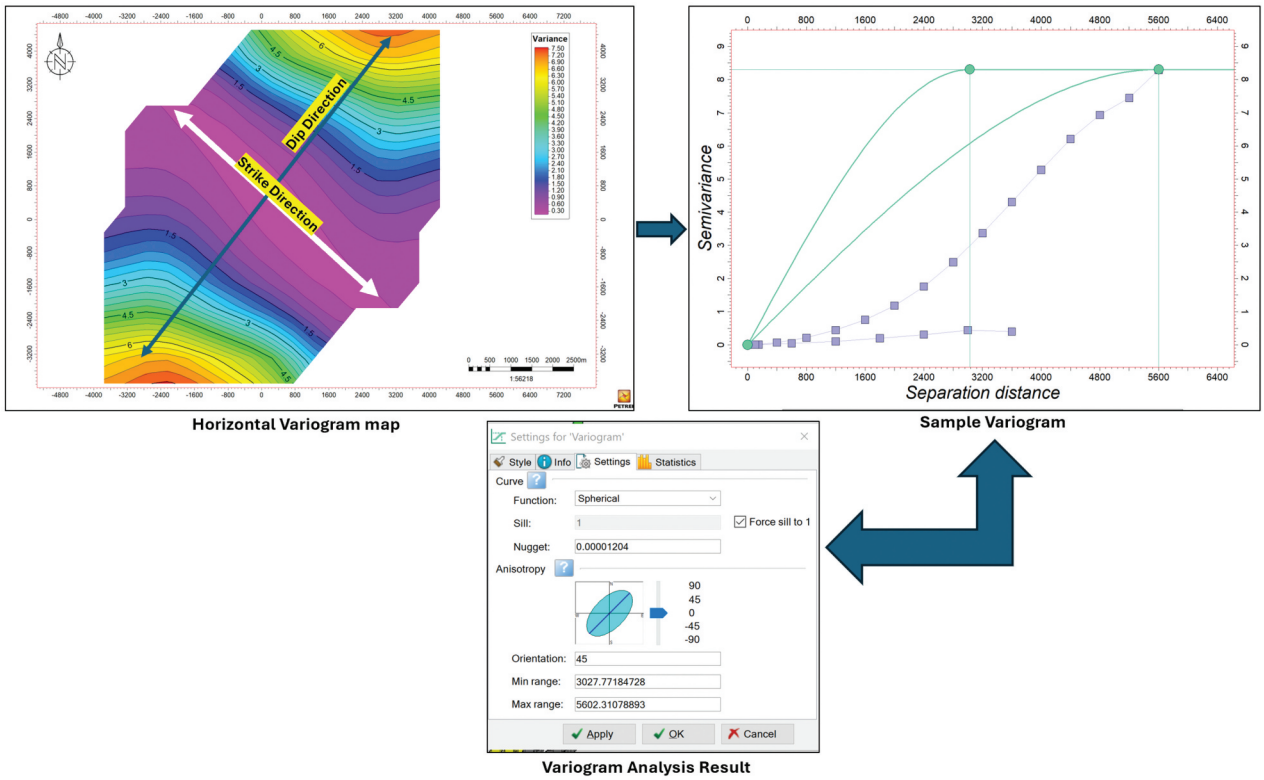

Figure 7. Horizontal Variogram Analysis.

grid cells before any modelling based on well logs can be done (Schlumberger 1989). This process is also called blocking of well logs. The scale-up of effective porosity, permeability, water saturation, NTG, and lithofacies was done and they serve as starting input into the facies and petrophysical modelling of the eleven hydrocarbon-bearing reservoirs within the Doma field.

3.14. Electro-facies modelling

Facies logs were generated for all Doma wells by deriving shale and sand facies from Vshale curves based on a cut-off of 0.4. The cut-off value was derived from a cross plot of Vshale Vs. effective porosity (Figure 8). Generated facies logs were upscaled to place average values into the cells along the wellbore. Data analysis was carried out to QC and prepare inputs for facies modelling. This involves (1) Analysis of the distribution of facies vertically through the Doma field model and (2) Analysis of the distribution in the thickness of facies bodies. Finally, facies were interpolated using the Sequential Indicator Simulation (SIS) algorithm. The Sequential Indicator Simulation (SIS) is a variogram-based categorical simulation technique which is implemented in most commercial software for geostatistical modelling. SIS is appropriate when there is no clear geological body geometry, and the spatial continuity is well described by variograms, for example, in highly diagenetically altered facies. Vertical proportion curves and variogram analysis results were incorporated to distribute the facies between wells across the area of interest.

3.15. Property and petrophysical modelling

The process of populating grid cells with discrete (facies) or continuous properties (i.e. porosity, permeability, and water saturation) once the geometric framework of the reservoir has been validated. The continuous properties were constrained to the facies model. The upscaled porosity curves (NTG, PhiT, PhiE & PermX) were modelled between cells using Sequential Gaussian Simulation (SGS) which is a computer-based algorithm that generates realisations from a multiGaussian random function. It is commonly used in a geostatistical simulation for reservoir modelling to model continuous variables like porosity. SGS generates multiple equally probable realisations of a property, which can be used to quantify and assess uncertainty. This is different from the Kriging algorithm, which estimates the mean. SGS adds back in variability to undo the smoothing effect of kriging, which may provide a better representation of the natural variability of the property. Water saturation was distributed using the saturation height function established from petrophysical evaluation parameters to compensate for the capillary pressure build-up and to account for the transition zone between 100% water zone and hydrocarbon zone. An exponential variogram with ranges of 5600 m and 3000 m, as derived from horizontal variogram analysis discussed in the previous section, and 10 ft vertical was adopted for use in the property distribution.

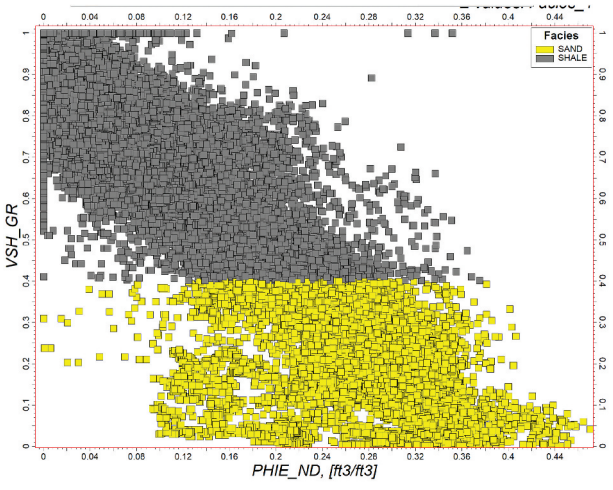

Figure 8. Electro-facies classification/definition.

3.16. Volumetrics

Reservoir fluid volumes were estimated from the geological models, based on the contacts defined in the model. The 3D stochastic model allows the dependencies between the various input parameters to be treated realistically and provides information on the spatial variability of the uncertainty. Gross rock volume calculations and Petrophysical parameters were used as input in the equation below for the estimation of oil originally in place, using all the water saturation modelling scenarios:

$$STOOIP = GRV * NTG * \Phi * (1 - Sw) * (1/Bo)$$

$$GIIP = GRV * NTG * \Phi * (1 - Sw) * (1/Bg)$$

Hydrocarbon volumetric uncertainty analysis was carried out by varying porosity and water saturation parameters using the uncertainty module in Petrel software. By varying these parameters, low, mid and high case volumes of hydrocarbon in place within the Doma field were generated. The computed volume and other parameters for the 1-IB2, 2-IB2, 3-IB2, 4-IB2, 10-IB2, 14-IB2, 1-IB1, 2-IB1, 3-IB1, 4-IB1 and 5-IB1 reservoirs are shown in Table 1.

3.17. Quantification of heterogeneity

A basic statistical tool was deployed in the quantification of heterogeneity from the computed and modelled petrophysical parameters within the study area.

Table 1. Showing Hydrocarbon Volume computed in the Doma field.

DOMA 01 PETROPHYSICAL SUMMARIES

Zones	Flag Name	Top	Bottom	Gross (ft)	Net (ft)	NTG	Av_PHIE (v/v)	Av_SW (v/v)
1-IB1	ROCK	5737.566	5766.176	28.610	19.263	0.673	0.282	0.241
1-IB1	RES	5737.566	5766.176	28.610	19.263	0.673	0.282	0.241
1-IB1	PAY	5737.566	5766.176	28.610	19.263	0.673	0.282	0.241
2-IB1	ROCK	5794.737	5829.575	34.838	29.185	0.838	0.316	0.243
2-IB1	RES	5794.737	5829.575	34.838	29.185	0.838	0.316	0.243
2-IB1	PAY	5794.737	5829.575	34.838	29.185	0.838	0.316	0.243
3-IB1	ROCK	6134.892	6179.051	44.159	2.478	0.056	0.321	0.255
3-IB1	RES	6134.892	6179.051	44.159	2.478	0.056	0.321	0.255
3-IB1	PAY	6134.892	6179.051	44.159	2.478	0.056	0.321	0.255
4-IB1	ROCK	6303.089	6387.367	84.278	71.336	0.846	0.343	0.199
4-IB1	RES	6303.089	6387.367	84.278	67.585	0.802	0.343	0.199
4-IB1	PAY	6303.089	6387.367	84.278	67.585	0.802	0.343	0.199
5-IB1	ROCK	6448.016	6498.913	50.897	14.735	0.290	0.286	0.587
5-IB1	RES	6448.016	6498.913	50.897	14.735	0.290	0.286	0.587
5-IB1	PAY	6448.016	6498.913	50.897	10.521	0.207	0.298	0.457

DOMA 01ST2 PETROPHYSICAL SUMMARIES

Zones	Flag Name	Top	Bottom	Gross (FT)	Net (FT)	NTG	Av_PHIE (v/v)	Av_SW (v/v)
1-IB1	ROCK	5655.635	5682.816	27.182	20.534	0.755	0.265	0.340
1-IB1	RES	5655.635	5682.816	27.182	20.534	0.755	0.265	0.340
1-IB1	PAY	5655.635	5682.816	27.182	18.254	0.672	0.280	0.297
2-IB1	ROCK	5710.026	5744.040	34.014	28.930	0.851	0.319	0.364
2-IB1	RES	5710.026	5744.040	34.014	28.930	0.851	0.319	0.364
2-IB1	PAY	5710.026	5744.040	34.014	28.930	0.851	0.319	0.364
3-IB1	ROCK	6030.253	6073.416	43.163	3.106	0.072	0.300	0.424
3-IB1	RES	6030.253	6073.416	43.163	3.106	0.072	0.300	0.424
3-IB1	PAY	6030.253	6073.416	43.163	2.330	0.054	0.324	0.344
4-IB1	ROCK	6189.464	6271.069	81.605	69.666	0.854	0.339	0.221
4-IB1	RES	6189.464	6271.069	81.605	61.842	0.758	0.339	0.221
4-IB1	PAY	6189.464	6271.069	81.605	61.061	0.748	0.341	0.217
5-IB1	ROCK	6326.421	6374.131	47.709	21.260	0.446	0.265	0.600
5-IB1	RES	6326.421	6374.131	47.709	21.260	0.446	0.265	0.600
5-IB1	PAY	6326.421	6374.131	47.709	15.743	0.330	0.272	0.479

DOMA 02 PETROPHYSICAL SUMMARIES

Zones	Flag Name	Top	Bottom	Gross (ft)	Net (ft)	NTG	Av_PHIE (v/v)	Av_SW (v/v)
1-IB2	ROCK	4095.764	4110.546	14.782	9.144	0.619	0.326	0.184
1-IB2	RES	4095.764	4110.546	14.782	9.144	0.619	0.326	0.184
1-IB2	PAY	4095.764	4110.546	14.782	9.144	0.619	0.326	0.184
2-IB2	ROCK	4122.505	4151.089	28.584	23.700	0.829	0.399	0.105
2-IB2	RES	4122.505	4151.089	28.584	23.700	0.829	0.399	0.105
2-IB2	PAY	4122.505	4151.089	28.584	23.700	0.829	0.399	0.105
3-IB2	ROCK	4220.658	4265.392	44.734	13.834	0.309	0.342	0.313
3-IB2	RES	4220.658	4265.392	44.734	13.834	0.309	0.342	0.313
3-IB2	PAY	4220.658	4265.392	44.734	13.834	0.309	0.342	0.313
4-IB2	ROCK	4496.711	4526.016	29.305	14.257	0.487	0.320	0.358
4-IB2	RES	4496.711	4526.016	29.305	14.257	0.487	0.320	0.358
4-IB2	PAY	4496.711	4526.016	29.305	14.257	0.487	0.320	0.358
10-IB2	ROCK	5154.640	5182.615	27.976	1.507	0.054	0.294	0.301
10-IB2	RES	5154.640	5182.615	27.976	1.507	0.054	0.294	0.301
10-IB2	PAY	5154.640	5182.615	27.976	1.507	0.054	0.294	0.301
14-IB2	ROCK	5663.271	5696.997	33.725	8.663	0.257	0.274	0.199
14-IB2	RES	5663.271	5696.997	33.725	8.663	0.257	0.274	0.199
14-IB2	PAY	5663.271	5696.997	33.725	8.663	0.257	0.274	0.199
3-IB1	ROCK	6306.849	6355.401	48.552	1.126	0.023	0.281	0.347
3-IB1	RES	6306.849	6355.401	48.552	1.126	0.023	0.281	0.347
3-IB1	PAY	6306.849	6355.401	48.552	1.126	0.023	0.281	0.347

DOMA 02 ST PETROPHYSICAL SUMMARIES

Zones	Flag Name	Top	Bottom	Gross (ft)	Net (ft)	NTG	Av_PHIE (v/v)	Av_SW (v/v)
1-IB2	ROCK	3903.602	3925.080	21.477	17.494	0.815	0.287	0.250
1-IB2	RES	3903.602	3925.080	21.477	15.495	0.721	0.287	0.250
1-IB2	PAY	3903.602	3925.080	21.477	15.495	0.721	0.287	0.250
2-IB2	ROCK	3936.076	3962.069	25.993	25.543	0.983	0.435	0.118
2-IB2	RES	3936.076	3962.069	25.993	23.794	0.915	0.430	0.125
2-IB2	PAY	3936.076	3962.069	25.993	22.744	0.875	0.433	0.095
3-IB2	ROCK	4034.277	4081.799	47.522	19.247	0.405	0.290	0.403
3-IB2	RES	4034.277	4081.799	47.522	19.247	0.405	0.290	0.403
3-IB2	PAY	4034.277	4081.799	47.522	16.247	0.342	0.312	0.347
4-IB2	ROCK	4318.238	4337.447	19.208	11.727	0.611	0.296	0.485
4-IB2	RES	4318.238	4337.447	19.208	11.727	0.611	0.296	0.485
4-IB2	PAY	4318.238	4337.447	19.208	9.499	0.495	0.292	0.393
10-IB2	ROCK	4990.740	5037.317	46.577	28.150	0.604	0.271	0.362
10-IB2	RES	4990.740	5037.317	46.577	28.150	0.604	0.271	0.362
10-IB2	PAY	4990.740	5037.317	46.577	23.749	0.510	0.283	0.290
14-IB2	ROCK	5527.777	5561.045	33.268	31.746	0.954	0.208	0.589
14-IB2	RES	5527.777	5561.045	33.268	29.247	0.879	0.219	0.577
14-IB2	PAY	5527.777	5561.045	33.268	19.248	0.579	0.241	0.481
3-IB1	ROCK	6236.829	6298.609	61.780	45.349	0.734	0.230	0.630
3-IB1	RES	6236.829	6298.609	61.780	44.099	0.714	0.234	0.626
3-IB1	PAY	6236.829	6298.609	61.780	25.746	0.417	0.261	0.501

The statistical tool used in the quantification of heterogeneity is the coefficient of variation. The coefficient of variation (CV) is a measure of variability relative to the mean value. A homogeneous formation will have a co-efficient variation of zero, with the value increasing with heterogeneity in the dataset (Elkateb et al. 2003). The input for the quantification of heterogeneity using the coefficient of variation method deduced from the equation is the mean and the standard deviation.

4. Results

4.1. Structural seismic interpretation

The interpretation of seismic data provides a deep understanding of the structural architecture and geometry of the subsurface reservoirs in the Doma field. The Seismic interpretation was carried out step by step following the methodology highlighted above for an easy and detailed understanding of the structural configuration of the Doma field.

The variance edge and structural smoothening volume seismic attribute previously discussed in Figure 5b above indicated that systems of two parallel oriented faults characterise the Doma field. The two major Faults are trending NE-SW and are both dipping south-eastern direction. Both faults run through the entire field thereby creating compartmentalisation within the field. The F1 fault extends laterally and vertically from reservoir 1-IB2 to 5-IB1. The crest of the structure collapsed against the F1. Other minor intraformational faults exist in the deeper reservoir from reservoir 1-IB1 to 5-IB1. They are intra-fault and thus did not form any compartmentalisation of the reservoirs. The parallel relationship of F1 and F2 is sustained in all reservoir levels within the Doma field. These faults are interpreted as normal faults and are listric in nature indicating Syn-depositional extensive tectonic regime. The faults F1 and F2 trending NE-SW break up the field into North-Western and South-Eastern flanks and they control the major compartmentalisation within the field. The North-Western flank is the only area where wells were drilled, thereby limiting interpretation and analysis to this region of Doma Field (Figure 5) above.

4.1.1. Horizon interpretation

The well correlation panel shows eleven (11) hydrocarbon-bearing sands were correlated across wells. These sand tops were tied to seismic during the seismic to well ties discussed above and were subsequently mapped across the entire seismic volume as discussed above. All eleven interpreted horizons displayed the structural framework and the faulting pattern of the study area. Fault Patterns were seen to be consistent in horizons 1-IB2 to 14-IB2 (Figure 5) since the

interpreted seismic events are not far from each other. Also, the fault pattern observed in horizon 1–IB1–5-IB1 is similar (Figure 5). Relationships exist between the generated time maps of the interpreted horizons and the converted depth maps as there are no observable changes in the structure (Figure 5).

4.1.2. Petrophysical analysis

The wells, Doma 1, Doma 1st2, Doma 2, Doma 2st, and Doma 2st2 were drilled to a total depth of 10,500 ft 10,463 ft 10,219 ft, 8316 ft, and 15,300 ft TD, respectively. The Doma 1 and Doma 2 are wildcat while Doma 1st2, Doma 2st1, and Doma 2st2 were appraisal wells. They all contain basic suites of well logs that were used in this research. Twenty-two (22) reservoirs from 1-IB2 to 5-IB1 were identified and correlated across the wells to establish the lateral continuity of the sand body package and their thickness/vertical variation within the field. These reservoirs were identified and correlated based on the GR, ILD and N-D log signature. Sand and Shale baseline of 70API was identified to distinguish sand from shale lithology. GR reading lower than 70API is interpreted as sand lithology while greater than 70API is interpreted as shale lithology. Sand lithology that has a corresponding ILD greater than 1.5ohms is interpreted as hydrocarbon-bearing sand, while those with ILD less than 1.5 ohms is interpreted as water-bearing sand. The neutron-density crossover was used in delineating hydrocarbon-bearing sand into oil and gas-bearing. The Reservoirs 1-IB2-14-IB2 were seen by Doma 2 and Doma 2st2, while reservoirs 1-IB1-5-IB1 were penetrated by all the wells within the field. The net sand thickness varied from 9.06 ft in 5-IB2 in Doma 02 to 64 ft in 4-IB1 in Doma 01. Reservoir 10-IB2, 14-IB2, 1-IB1, and 2-IB1 were all oil bearing, reservoir 1-IB2, 2-IB2, 3-IB2, 4-IB1, and 5-IB1 are gas bearing while 4-IB2, and 3-IB1 contain both oil and gas. Doma 01 well saw ODT in reservoir 1-IB1 and 2-IB1 at 5766 ft, 5829 ft SSTVD while Doma 1st2 saw ODT in 1-IB1 and 2-IB1 at 5682 ft and 5744 ft TVDSS, respectively. Doma 02 saw ODT in 10-IB2 and 14-IB2 at 5183 ft and 5697 ft TVDSS. Doma 01 saw GDT in 4-IB1 and 5-IB1 at 6387 ft and 6499 ft TVDSS while Doma 1st2 saw GDT in 4-IB1 and 5-IB1 at 6189 ft and 6374 ft TVDSS, respectively. Doma 02 and Doma 02st saw GDT in 3-IB2 at 4265 ft and 4081 ft TVDSS, respectively, and Doma 02 saw GOC and OWC at 4504 ft and 4523 ft TVDSS in 4-IB2 reservoir, respectively. Reservoirs 1-IB1, 2-IB1, 4-IB1 & 5-IB1 are wet in Doma 02 ST1 and Doma 02. The evaluation log plot of some of the hydrocarbon-bearing reservoirs is displayed in Figure 4.

The effective porosity values within the Doma field range from 24% in sand 14-IB2 to 33% in sand 2-IB2 sands while NTG ranges from 31% in 3-IB2 to 92% in 2-IB2 reservoir. The values of water saturation computed range from 11% in 2-IB2 to 50% in 3-IB1 reservoir. Table 2 shows petrophysical summaries of Doma field wells.

5. Discussion

5.1. Geological reservoir modelling

5.1.1. Structural and Stratigraphic Models

The structural models reveal that the reservoirs within the Doma field build and collapse towards the Northeast-Southwestern trending major fault that dips south-eastern direction (Figure 6). The major (regional) growth fault is elongated along NE-SW trending faults that assisted the reservoir dip closure in trapping the reservoir oil. The vertical stratigraphic sequence of the reservoirs in the Doma field depicts

Table 2. Showing Petrophysical Summaries for Doma Field wells.

Reservoir	FLUID	OIL (MMSTB)			GAS (BCF)		
		LOW	MID	HIGH	LOW	MID	HIGH
1-IB2	GAS				6.34	8.41	10.36
2-IB2	GAS				11.14	14.79	18.21
3-IB2	GAS				12.72	16.60	20.95
4-IB2 GAS	GAS				0.59	0.76	0.94
4-IB2	OIL	2.47	3.18	3.96			
10-IB2	OIL	3.37	4.36	5.45			
14-IB2	OIL	10.87	14.09	17.65			
1-IB1	OIL	8.23	10.86	13.89			
2-IB1	OIL	12.56	16.49	20.96			
3-IB1 GAS	GAS				10.46	13.22	16.09
3-IB1	OIL	6.13	7.75	9.43			
4-IB1	GAS				25.87	34.35	44.19
5-IB1	GAS				6.54	8.18	9.84
	Total	43.63	56.72	71.34	73.65	96.30	120.59

a marine regression. Based on the GR log motifs, the reservoir sand depicts a coastal deltaic progradation with a coarsening upward para-sequence architecture. The major fault within the field is extensive and is cut across all the hydrocarbon-bearing reservoirs from 1–IB2–5-IB1. The other faults within the field are minor in nature and aid compartmentalisation in reservoirs 1-IB1, 2-IB1, and 3-IB1. The structural modelling of the Doma field thereby conforms with and validates the structural configuration of the field that was obtained from the depth grid maps during seismic interpretation.

5.1.2. Facies modelling

The views of the lithological/electro-facies/rock type model of reservoirs 1-IB2, 2-IB2, 3-IB2, 4-IB2, 10-IB2, and 14-IB2 are displayed in Figure 9. The electrofacies/rock-type models revealed the lateral distribution of sand and shale Electro-facies within the Doma field. Laterally, it is evident in Figure 9 that reservoir 2-IB2 has better sand distribution indicating there are more sand rock types while 3-IB2 has the highest shale facies suggesting that there is more shale rock type within the reservoir. The percentage sand electro-facies are in the order from reservoir 2-IB2, 14-IB2, 1-IB1, 4-IB1, 2-IB1, 3-IB1, 4-IB2, 5-IB1, 10-IB2, 1-IB2 and least in 3-IB2. Only reservoir 2-IB2 has excellent sand lithology distribution across the entire Doma field indicating that the reservoir will most likely have excellent porosity and permeability properties which are rock types-based parameters.

5.1.3. Petrophysical Property Modelling

The modelled reservoir's porosity, permeability, and net-to-gross ratios are usually good, except for the southern and eastern regions, which exhibit significant variation and variability. PHIT models are displayed in Figure 10, PHIE is displayed in Figure 11, NTG models are displayed in Figure 12, permeability models are displayed in Figure 13, and water saturation models are displayed in Figure 14. The average effective

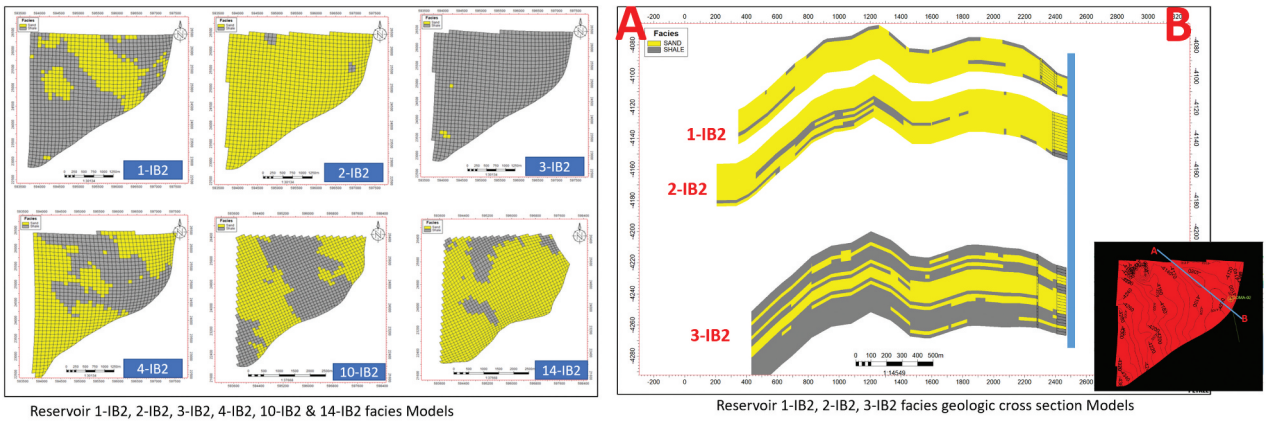

Reservoir 1-IB2, 2-IB2, 3-IB2, 4-IB2, 10-IB2 & 14-IB2 facies Models

Reservoir 1-IB2, 2-IB2, 3-IB2 facies geologic cross section Models

Figure 9. Reservoir 1-IB2, 2-IB2, 3-IB2, 4-IB2, 10-IB2 & 14-IB2 facies Models and geologic cross sections.

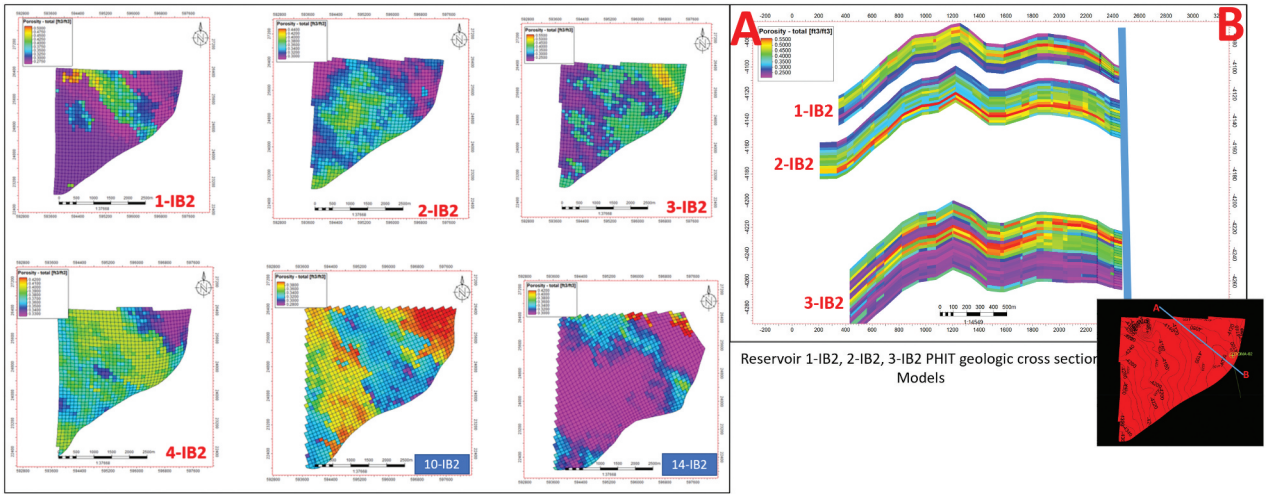

Reservoir 1-IB2, 2-IB2, 3-IB2, 4-IB2, 10-IB2 & 14-IB2 PHIT Models

Reservoir 1-IB2, 2-IB2, 3-IB2 PHIT geologic cross section Models

Figure 10. Reservoir 1-IB2, 2-IB2, 3-IB2, 4-IB2, 10-IB2 & 14-IB2 PHIT Models and geologic cross sections.

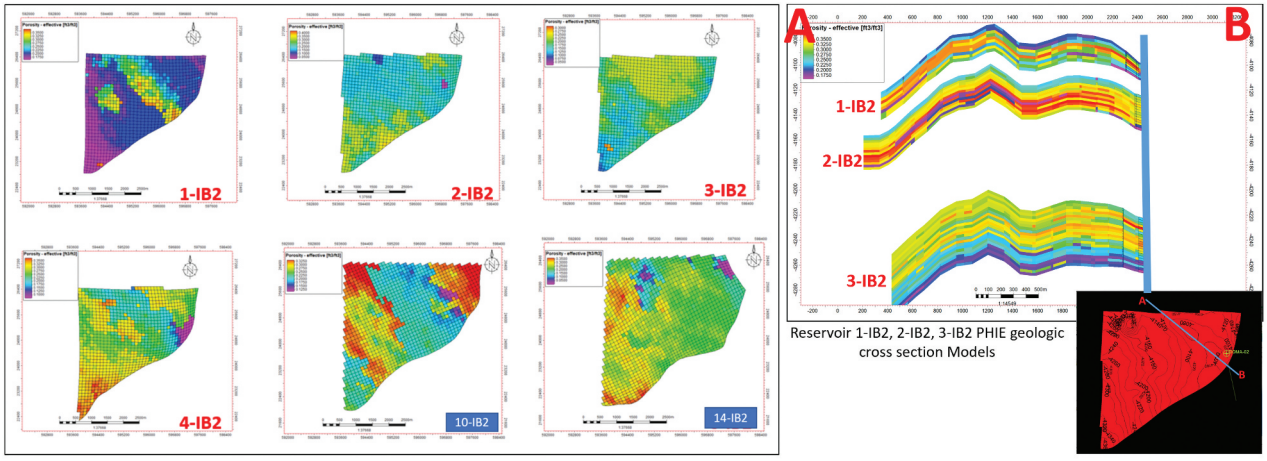

Figure 11. Reservoir 1-IB2, 2-IB2, 3-IB2, 4-IB2, 10-IB2 & 14-IB2 PHIE Models and geologic cross sections.

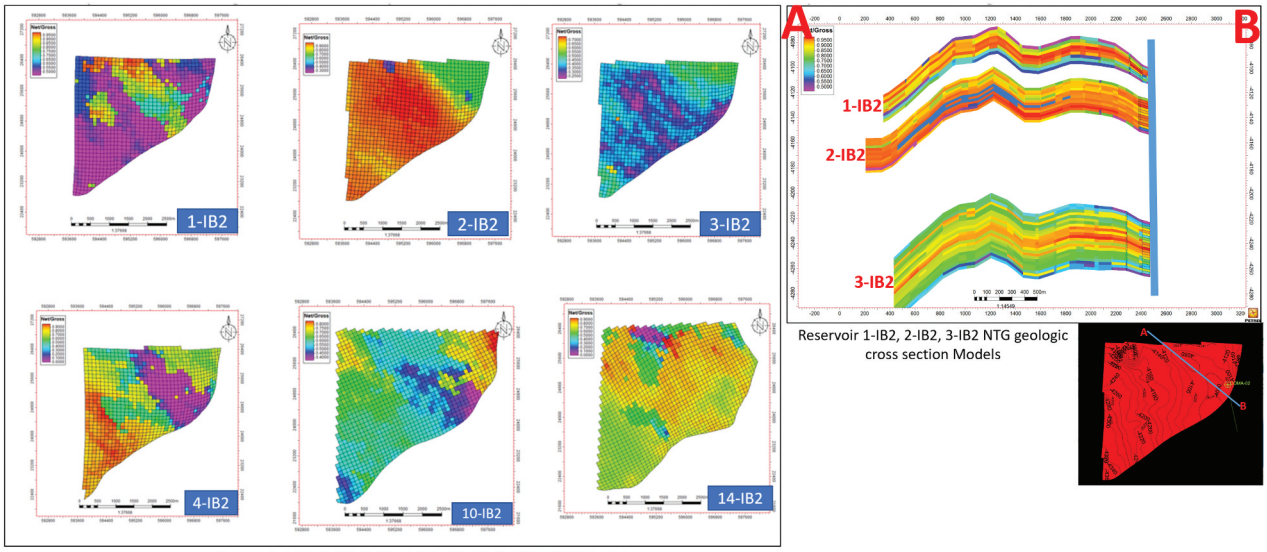

Figure 12. Reservoir 1-IB2, 2-IB2, 3-IB2, 4-IB2, 10-IB2 & 14-IB2 NTG Models and geologic cross sections.

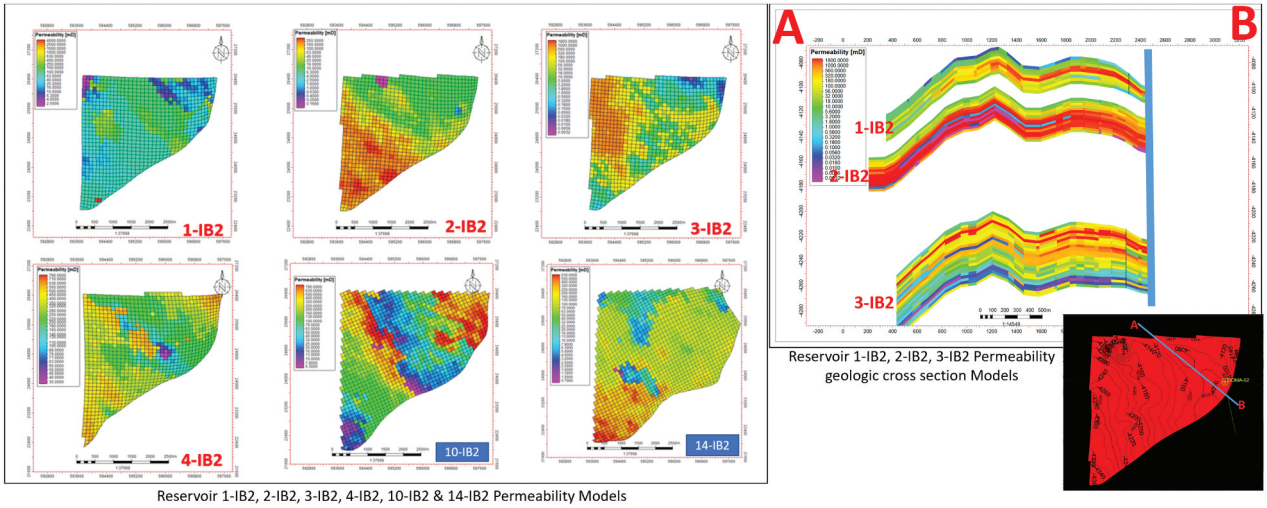

Figure 13. Reservoir 1-IB2, 2-IB2, 3-IB2, 4-IB2, 10-IB2 & 14-IB2 Permeability Models and geologic cross sections.

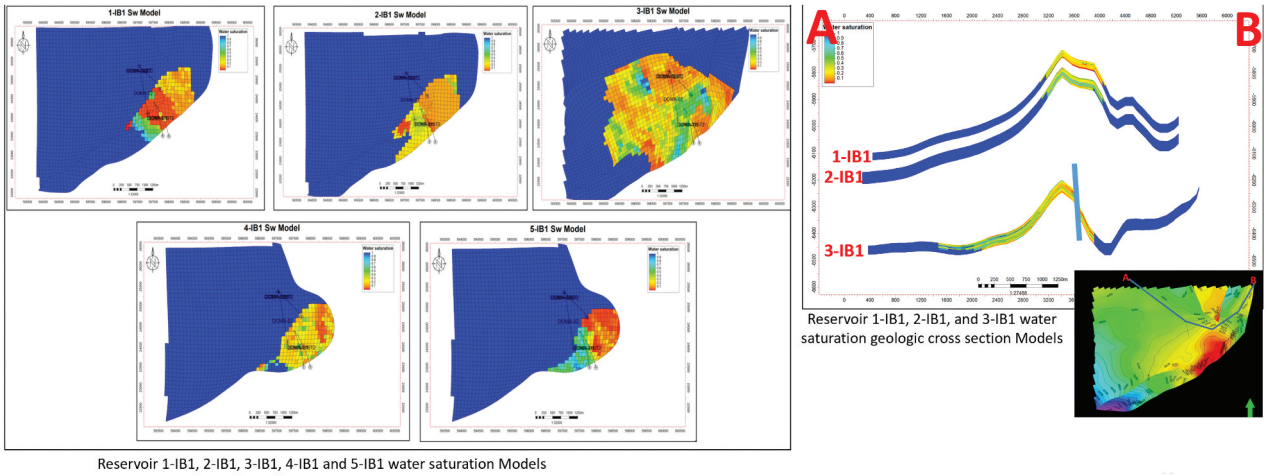

Figure 14. Reservoir 1-IB2, 2-IB2, 3-IB2, 4-IB2, 10-IB2 & 14-IB2 Water Saturation Models and geologic cross sections.

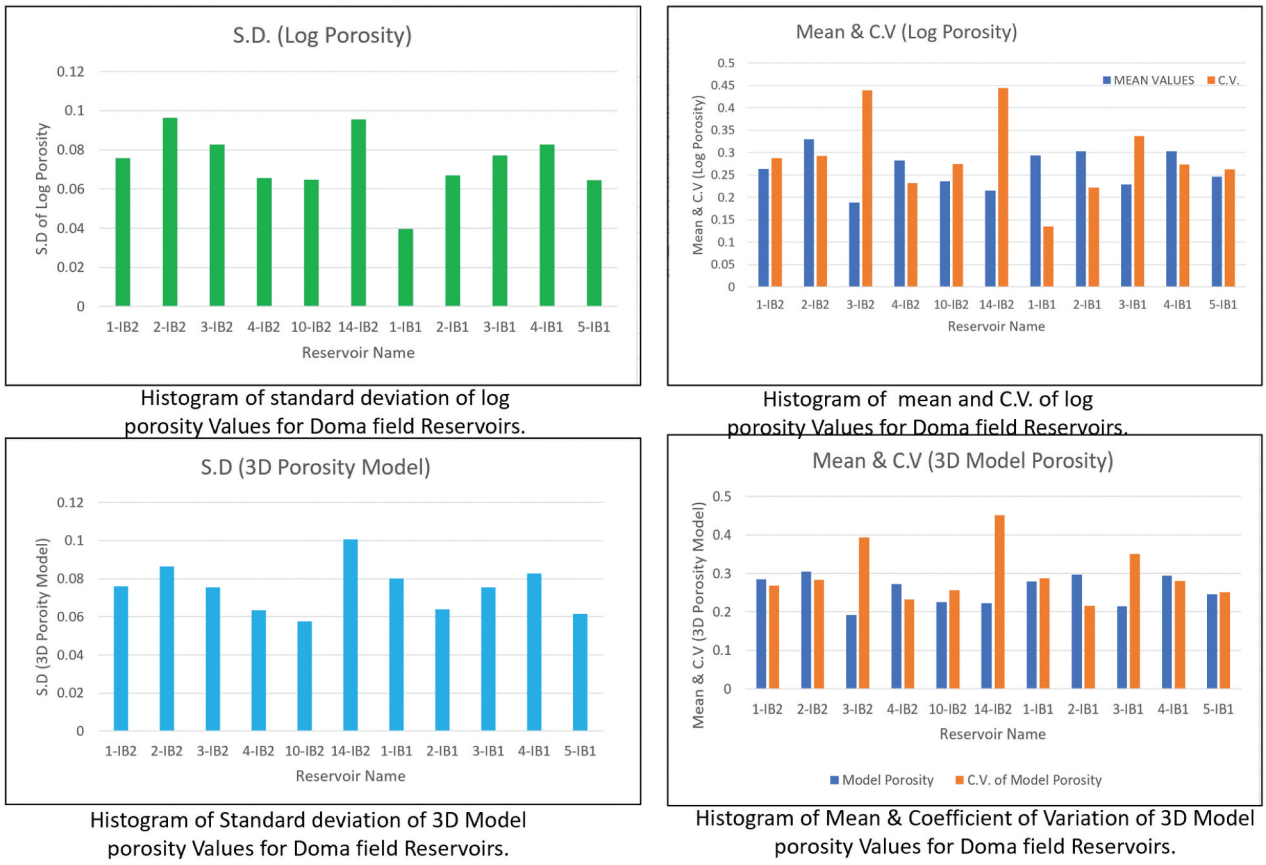

Figure 15. Showing Coefficient of Variation of Hydrocarbon bearing reservoir in Doma field.

porosity ranges between 20% and 40% while the model permeability is greater than 0.1mD indicating that the reservoirs within the Doma field have excellent pore spaces that are interconnected, which is required for easy transmission/mobility of hydrocarbon into the producer well during the production stage.

5.2. Volumetric computation

Hydrocarbon volumes estimated from the 3D reservoir models for all the hydrocarbon-bearing reservoirs in the Doma field are displayed in Table 1 and it shows that reservoir 4-IB2 has the lowest STOIP of 3MMSTB of oil, while reservoir 2-IB2 has the highest STOIP of

16MMSTB of oil. Reservoir 4-IB1 has the highest gas in place of 34.35 BSCF, while 4-IB2 has the lowest GIIP of 0.76 BSCF. Based on uncertainty analysis, the low case, base case, and high case cumulative volumetric for oil is 43.63MMSTB, 56.72MMSTB, and 71.34MMSTB and gas is 73.65BSCF, 96.3BSCF, and 120.59BSCF, respectively. Table 1 shows these hydrocarbon volume in the Doma field.

5.3. Quantification and classification of reservoir heterogeneity

To quantify and classify the heterogeneous nature of reservoirs within the Doma field, the basic statistical tool was adopted as discussed above. The coefficient of variation of log-derived porosity from petrophysical analysis and 3D geological reservoir model are presented in Figure 15. The coefficient of variation computed from log-derived porosity varies from 0.14 in reservoir 1-IB1 to 0.44 in reservoir 14-IB2. While the coefficient of variation computed from the 3D model porosity varies from 0.21 in reservoir 2-IB1 to 0.45 in reservoir 14-IB2 (Figure 15). These values suggested that the Doma field is characterised by weak to medium intra-formational heterogeneity with reservoir 1-IB1 being least heterogenous and 14-IB2 being the most heterogenous within the field.

6. Conclusion

The integrated reservoir characterisation and 3D geological reservoir trend modelling of rock properties utilising well-logs and seismic data for 3D architectural sand body geometry and heterogeneity delineation, geological reservoir trend modelling, quantification of heterogeneity, and assessment of hydrocarbon beyond well control within the Doma field have been done. This research has further buttressed the efficacy of well and seismic data integration in 3D geological reservoir modelling operations. Also, the study has shown the application of statistical tools in quantifying reservoir model heterogeneity and thus created a reference model for siliciclastic reservoir heterogeneity classification in the Niger Delta area. The low case, base case, and high case cumulative volumetric for oil is 43.63MMSTB, 56.72MMSTB, and 71.34MMSTB, and for gas is 73.65BSCF, 96.3BSCF, and 120.59BSCF, respectively, which indicated that Doma field contains hydrocarbon that can be produced in commercial quantity. The application of a statistical tool (coefficient of variation) for the quantification of the reservoir heterogeneity revealed a weak to medium heterogeneous classification of the Doma field.

Disclosure statement

No potential conflict of interest was reported by the author(s).

ORCID

Gabriel Efomeh Omolaiye http://orcid.org/0000-0001-7598-2422

Abbreviations

GR	Gamma Ra Log
ILD	Induction Resistivity
NPHI	Neutron Porosity
RHOB	Bulk Density
PHIT	Total Porosity
NTG	Net-to-Gross
Sw	Water Saturation
PHIE	Effective Porosity
STOIP	Stock Tank Oil Initially In Place
GIIP	Gas initially In-Place
MMSTB	million Stock Tank Barell
BSCF	Billion Standard Cubic Feet
3D	Three Dimensional
mD	Milli Darcies.
ST	Side Track
SSTVD	Sub Sea True Vertical Depth
ODT	Oil-Down-To
GDT	Gas-Down-To
GOC	Gas oil Contact
OWC	Oil-Water-Contact
GRV	Gross Rock Volume
Φ	Porosity
Bo	Oil formation volume factor
Bg	Gas formation volume factor
SGS	Sequential Gaussian Simulation
SIS	Sequential Indicator Simulation
API	Aerican Petroleum Institute
N-D	Neutron – Density

References

Adepelumi AA, Hammed O, Afe M. 2018. Application of 3D geological reservoir modeling in hydrocarbon volumetrics and production performance enhancement of XYZ field, Niger Delta. Paper Presented at Nigerian Association of Petroleum Explorationists 2018 Annual Conference and Exhibition in Eko Hotel & Suites; Lagos, Nigeria.

Agharanya PU, Ekwenye OC, Okogbue CO, Mode AW, Okeke KK. 2022. Stratigraphic palynology and micropaleontological study of the cretaceous-paleogene succession of the Nani-1 well of the anambra and niger delta basins: Implications for hydrocarbon exploration. J Afr Earth Sci. 195:104637. doi: 10.1016/j.jafrearsci.2022.104637.

Allen JRL. 1965. Late Quaternary Niger Delta and adjacent areas: sedimentary environment and lithofacies. Am Assoc Petroleum Geologists. 49:549–600. doi: 10.1306/A663363A-16C0-11D7-8645000102C1865D.

Barton MD, Fisher RS, Tyler N. 1992. Quantifying Reservoir Heterogeneity through outcrop characterization: Architecture, Lithology, and permeability distribution of a landward -stepping fluvial – deltaic sequence, Ferron sandstone (cretaceous), central Utah. Topical Report GRI-93/0022. 1–150.

Bedle H, Chopra S, Davis T. 2024. Introduction to this special section: Reservoir Characterization. Leading Edge, pg 43(12):798–799. doi: 10.1190/tle43120798.1.

Correia U, Batezelli A, Leite E. 2016. 3-D Geological modelling: A siliciclastic reservoir case study from Campos Basin, Brazil. REM, Int Eng J. 69(4):409–416. doi: 10.1590/0370-44672015690063.

De Ros LF, Zuffa GG, Morad S. 1998. Heterogeneous generation and evolution of diagenetic quartzarenites in the Silurian-Devonian Furnas Formation of the Paraná Basin, southern Brazil. South BrazilSedimentary Geol. 116(1–2):99–128. doi: 10.1016/S0037-0738(97)00081-X.

Doust H, Omatsola E. 1989. Niger Delta. Am Assoc Petroleum Geologists Mem. 48:201–238.

Doust H, Omatsola E. 1990. Niger Delta. In: Edwards JD, and Santogrossi PA, editors. Divergent/Passive Margin Basins Vol. 48, USA: American Association of Petroleum Geologists; p. 239–248.

Dykstra H, Parsons RL. 1950. The Prediction of Oil Recovery by Water Flood. Secondary Recovery of Oil in the United States: principles and Practice. (NY): American Petroleum Institute.

Ekwenye OC, Nichols G, Mode AW. 2015. Sedimentary petrology and provenance interpretation of the sandstone lithofacies of the Paleogene strata, south-eastern Nigeria. J Afr Earth Sci. 109:239–262. doi: 10.1016/j.jafrearsci.2015.05.024.

Elkateb T, Chalaturnyk R, Robertson P. 2003. An overview of soil heterogeneity: quantification and implications on geotechnical field problems. Can Geotech J. 40(1):1–15. doi: 10.1139/t02-090.

Evamy BD, Haremboure J, Kamerling P, Knaap WA, Molloy FA, Rowlands PH. 1978. Hydrocarbon habitat of tertiary Niger Delta. American Association of Petroleum. Geologists Bull. 62:277–298. doi: 10.1306/C1EA47ED-16C9-11D7-8645000102C1865D.

Ezekwe JN, Filler SL. 2005 Oct. Modelling Deepwater Reservoirs: A paper (SPE 95066). Presented at SPE Annual Technical Conference and Exhibition; Dallas, (TX), U.S.A., 9. p. –12.

Fitch PJR, Lovell MA, Davies S, Harvey P, Pritchard T. 2015. An integrated and quantitative approach to petrophysical heterogeneity. Mar Petroleum Geol. 63:82–96. doi: 10.1016/j.marpetgeo.2015.02.014.

Meldahl P, Heggland R, Bril B, de Groot P. 2001. Identifying faults and gas chimneys using multiattributes and neural networks. The Leading Edge. 20(5):474–482. doi: 10.1190/1.1438976.

Okeke KK, Umeji OP. 2016. Palynostratigraphy, palynofacies and palaeoenvironment of deposition of Selandian to Aquitanian sediments, southeastern Nigeria. J Afr Earth Sci. 120:102–124. doi: 10.1016/j.jafrearsci.2016.04.020.

Oladele S, Adepelumi A, Hammed O. 2020. Integrated 3d geological reservoir modeling for sand body geometry and heterogeneity delineation: implication for hydrocarbon potential assessment of "Gmedal" Field, Offshore, Niger Delta. NAPE Bull. 29(1):89–107.

Oomkens E. 1974. Lithofacies relations in the Late Quaternary Niger Delta complex. Sedimentology. 21 (2):195–222. doi: 10.1111/j.1365-3091.1974.tb02056.x.

Schlumberger. 1989. Petrel geology and Modelling 559. Petrel Introduction Course.

Schulz - Rojahn JP, Phillip SE. 1989. Diagenetic alteration of Permian reservoir sandstones in the Nappamerri Trough and adjacent areas, Southern Cooper Basin. O'Neil BJ editor. The Cooper and Eromanga Basins Australia: Proceedings of the Cooper and Eromanga Basins Conference, Adelaide. Petroleum Exploration Society of Australia, Adelaide, Society of Petroleum Engineers and Australian Society of Exploration Geophysicists (South Australian Branches). p. 629–645.

Sech RP, Jackson MD, Hampson GJ. 2009. Three-dimensional modeling of a shoreface-shelf parasequence reservoir analog: part 1. Surface-based modeling to capture high-resolution facies architecture. Bull Am Assoc Petrol Geol. 93(9):115–118. doi: 10.1306/05110908144.

Short KC, Stauble J. 1967. Outline geology of the Niger Delta. Am Assoc Petroleum Geologists Bull. 5:761–779.

Stacher P. 1995. Present understanding of the Niger Delta hydrocarbon habitat. In: Oti MN Postma G, editors. Geology of Deltas. Rotterdam: A.A. Balkema; p. 257–267.

Tuttle WLM, Charpentier RR, Brownfield ME. 1999 Open-file report 99-50-H. The Niger Delta petroleum system: niger Delta province, Nigeria, Cameroon and Equatorial Guinea, Africa. Denver (CO): USGS.

Weber KJ. 1987. Hydrocarbon distribution patterns in Nigerian growth fault structures controlled by structural style and stratigraphy. J Petroleum Sci Eng. 1(2):91–104. doi: 10.1016/0920-4105(87)90001-5.

Weber KJ, Daukoru EM. 1975. Petroleum Geology of the Niger Delta: Proceedings of the Ninth World Petroleum Congress. Geology; London: Applied Science Publishers, Ltd, volume 2. p. 210–221.

Weston L. 2024. The art of reservoir characterization. The Leading Edge pg 43(12):800–805. doi: 10.1190/tle43120800.1.